



Theoretical Estimation of Power Generation Performance of Nano-Sheet Planar Lateral P-N Junction under Illumination

Yasuhisa Omura^{1, 2*} 

¹Organization for Research and Development of Innovative Science and Technology, Kansai University, Suita, Osaka, Japan

²Academic Collaboration Associates, Kanagawa, Japan
E-mail: omuray@kansai-u.ac.jp

Received: March 05, 2023

Revised: March 25, 2023

Accepted: March 27, 2023

Abstract— This paper proposes covalent-semiconductor-based lateral p-n junction film solar devices based on a theoretical model, and examines their power generation performance under illumination. The proposed theoretical model is implemented and tested in simulations. The results demonstrate that while Ge film devices have much lower performance at room temperature than Si film devices, this order is significantly reversed at temperatures below 250 K, which is very interesting. The obtained simulation results also reveal that the carrier generation characteristic of Ge film devices is very stable in terms of temperature variation in comparison to Si film devices. The simulation results suggest that thin-Si-film lateral p-n junction solar devices - implemented as multi-stacked solar devices formed on a transparent panel - are applicable to field sensor devices on the ground at temperatures lower than 300 K. However, thin-Ge-film lateral p-n junction solar devices are applicable to field sensor devices on satellites in space because the ambient temperature is lower than 250 K; again as a multi-stacked solar device formed on a transparent panel.

Keywords— Lateral p-n junction film solar device; Si; Ge; Sensor network; Low-energy applications.

1. INTRODUCTION

The fundamental of semiconductor pn junctions was proposed by Shockley [1] and many theoretical reconsiderations [2, 3] and device applications [4] have been advanced in the last 70 years. Recently, electrostatic physics for the planar sheet pn junction structure has been theoretically reviewed [5, 6], and a very interesting discussion was advanced. The theory mathematically describes the influence of geometry on the reduction in the depletion region across the pn junction. This theoretical advance seems very important from the viewpoint of future thin-film device applications of various pn junction structures.

The author proposed a pn-junction-based optical rotor that operates under external illumination [7-10]. Though the device was proposed as a mechanical part for Micro Electro Mechanical System (MEMS) applications [11-15], its full potentiality has yet to be examined in experiments. The MEMS applications envisaged [16-18] must have very low-power operation because they must work with very small batteries, not with ac power supplies. It is in this background that piezoelectric micro power generators are being investigated [19], where performance of $\sim 0.01 \mu\text{J}/\text{cm}^3$ has been demonstrated. Since the energy density is still small for most applications, further investigation is needed. In order to advance the performance of such power supplies, the author proposed an advanced Schenkel circuit for RF-ID

* Corresponding author

applications [20], but the idea remained to be confirmed as practical for low-energy and high-frequency circuits and systems.

Flexible electronics technologies are now being applied to solar battery devices formed on various films [21-23] because they have high potential for future mobile battery [24-26] and medical implantation applications [27]. Though past proposals of lateral p-n junction solar battery devices have already been compared [28], chalcogenides have become the focus of attention [29-36].

In this paper, the author theoretically examines the photovoltaic performance of the covalent-semiconductor-based planar lateral pn junction sheet to correct the paucity of interest in and research of it. In this study, not vertical, but the lateral pn junction structure is the focus of attention [7-10]. The vertical pn junction structure is very fatally weak against local threading defects. On the other hand, the lateral pn junction structure is very robust against such local defects. In addition, our study demonstrated that performance of a lateral thin-film Si pn junction device is almost insensitive to minority carrier lifetime [9]. Therefore, it is expected that such lateral pn junction devices are still promising for various applications.

Though the primary theoretical base was given in [10], some additional theoretical concepts are introduced and numerically evaluated. Here, various calculations are performed for Si and Ge from the viewpoint of applications, and the potential for device application is discussed.

2. THEORETICAL BASE OF SIMULATIONS

A physical image of the planar lateral p-n junction sheet is shown in Fig. 1, where the top view of the device is given in Fig. 1(a); it is assumed that the green light illumination is vertical to the sheet's surface. This configuration is quite different from those of conventional solar cells. A practical layout for applications is shown in Fig. 1(b). Device parameters assumed here are summarized in Table 1. The following mathematical analyses are based on Boltzmann's statistics.

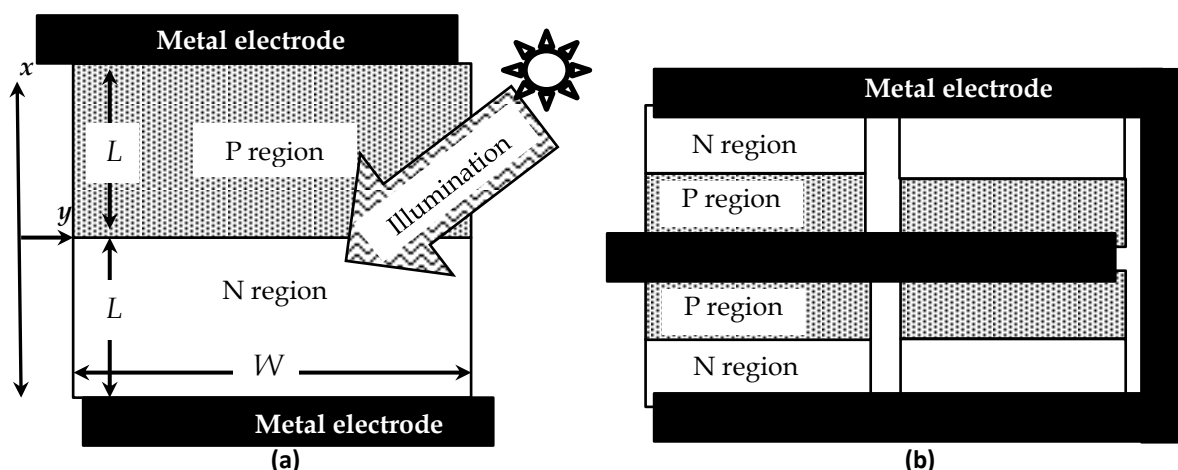


Fig. 1. Nanometer-thick planar lateral p-n junction sheet on an insulator: a) basic configuration of the device and assumptions; b) image of practical application layout.

The generation and recombination process of holes, for example, in the p-type region under illumination, generally follows the continuity equation given by:

$$\frac{\partial p_p(x,t)}{\partial t} = G_p - \frac{p_p(x,t) - p_{p0}}{\tau_p} - p_p \mu_p \frac{\partial F}{\partial x} - \mu_p F \frac{\partial p_p}{\partial x} + D_p \frac{\partial^2 p_p}{\partial x^2}. \quad (1)$$

where p_{p0} , G_p , τ_p , F , μ_p , and D_p denote the hole concentration at thermal equilibrium, the generation rate of holes, the lifetime of holes, the local electric field, hole mobility, and the diffusion constant of holes, respectively. A similar equation is made for electrons in the n-type region.

The local electric field follows Poisson's equations as shown below:

$$\begin{aligned} -\frac{\partial F}{\partial x} &= -\frac{q}{\epsilon_s} (p_p - p_{p0} - n_p + n_{p0}), \\ &\cong -\frac{q}{\epsilon_s} (p_p - N_A), \end{aligned} \quad (2)$$

where q is the magnitude of elemental charge, ϵ_s is the permittivity of the semiconductor, N_A is the acceptor concentration in the p-type region, n_p is the electron concentration under illumination in the p-type region, and n_{p0} is the electron concentration at thermal equilibrium. As we assume the local gradient of $(p_p - N_A)$ is not so large, we have:

$$F \cong \frac{q}{\epsilon_s} (p_p - N_A) L_{Dp}, \quad (3)$$

where L_{Dp} is the Debye length of the p-type region.

At steady state, we have:

$$G_p - \frac{p_p(x,t) - p_{p0}}{\tau_p} - p_p \mu_p \frac{\partial F}{\partial x} - \mu_p F \frac{\partial p_p}{\partial x} + D_p \frac{\partial^2 p_p}{\partial x^2} = 0. \quad (4)$$

Eq. (4) can be rewritten as:

$$D_p \frac{\partial^2 p_p}{\partial x^2} - \left(\frac{q L_{Dp} \mu_p}{\epsilon_s} \right) \left(2 p_p \frac{\partial p_p}{\partial x} - N_A \frac{\partial p_p}{\partial x} \right) - \frac{p_p(x,t) - N_A - G_p \tau_p}{\tau_p} = 0. \quad (5)$$

The expression for $p_p(x)$ is replaced with the following excess hole concentration $P(x)$.

$$P(x) = p_p(x) - N_A - G_p \tau_p. \quad (6)$$

After some approximations are applied to Eq. (5)[10], we get the following solution:

$$P(x) = \frac{2 \frac{\sqrt{2C_p}}{A_p} \frac{P(0)}{P(0) + 2 \frac{\sqrt{2C_p}}{A_p}} \exp(\sqrt{2C_p} x)}{1 - \frac{P(0)}{P(0) + 2 \frac{\sqrt{2C_p}}{A_p}} \exp(\sqrt{2C_p} x)} \quad (7)$$

$$P(0) = p_p(0) - N_A - G_p \tau_p, \quad (8)$$

$$A_p = \frac{2q L_{Dp} \mu_p}{D_p \epsilon_s}, \quad (9)$$

$$C_p = \frac{1}{D_p \tau_p}. \quad (10)$$

The theoretical expression for electrons in the n-type region is also written in similar algebra [10].

$$N(x) = \frac{2 \frac{\sqrt{2C_n}}{A_n} \frac{N(0)}{N(0) + 2 \frac{\sqrt{2C_n}}{A_n}} \exp(\sqrt{2C_n} x)}{1 - \frac{N(0)}{N(0) + 2 \frac{\sqrt{2C_n}}{A_n}} \exp(\sqrt{2C_n} x)} \quad (11)$$

$$N(0) = n_n(0) - N_D - G_n \tau_n, \quad (12)$$

$$A_n = \frac{2qL_{Dn}\mu_n}{D_n \epsilon_s}, \quad (13)$$

$$C_n = \frac{1}{D_n \tau_n}. \quad (14)$$

where each parameter with suffix 'n' is the counterpart of that in the n-type region.

This study assumes the external illumination source power (P_{ph}) is given as:

$$P_{ph} = N_{ph} h \frac{c}{\lambda}, \quad (15)$$

where c is the speed of light in a vacuum, λ is the wavelength, h is Planck's constant, and N_{ph} is the photon density. The carrier generation rate is given as:

$$G_n = G_p = \frac{N_{ph}}{t_s} (1 - R) l_c \left[1 - \exp\left(-\frac{t_s}{l_c}\right) \right], \quad (16)$$

where R is the reflection fraction and l_c is the absorption length.

Since the external illumination yields excess electrons and holes in the film, they yield the following terminal-to-terminal potential difference (V_{out}).

$$V_{out} = \left(\frac{q}{\epsilon_s} \right) \left[\int_{-L}^0 (N_D + N(x)) x dx + \int_0^L (N_A + P(x)) x dx \right] \quad (17)$$

In addition, the internal resistance (R_{int}) under illumination is given as:

$$R_{int} = \frac{L^2}{qWt_s \left[\mu_n \int_{-L}^0 (N_D + N(x)) dx + \mu_p \int_0^L (N_A + P(x)) dx \right]} \quad (18)$$

Using these calculation results, we can calculate, theoretically, the maximal voltage (V_{max}), the maximal load current (I_{max}), the efficiency, and fill factor [37], where temperature dependence of carrier mobility and band gap is given in the appendix.

3. CALCULATION RESULTS AND DISCUSSION

In this section, it is assumed that lateral sheet pn-junction devices are fabricated on a flexible film and glass. It is expected that those devices are applicable to wrist watches, IoT sensors, or satellites, making very low-energy operation systems essential. Therefore, it should be investigated whether the performance of the photovoltaic device satisfies the application requirements.

All simulations are performed using a home-made source code, not commercial software packages. Device parameters and physical parameters assumed here are summarized in Tables 1 and 2, respectively. The author's previous study demonstrated that the carrier generation and recombination process is insensitive to carrier lifetime values [9]. For simplicity, electrons and holes are assumed to have lifetimes of 10 ns.

Table 1. Parameters of the control device.

Parameters	Values	Units
Length of n-region and p-region (L)	1.0	μm
Width of n-region and p-region (W)	10.0	μm
Thickness (t_s)	100.0	nm
Doping level of n-region (N_D)	1.0×10^{15}	$/\text{cm}^3$
Doping level of p-region (N_A)	1.0×10^{15}	$/\text{cm}^3$

Table 2. Physical parameters of the control device.

Parameters	Values	Unit
Lifetime of electrons (τ_{n0})	10.0	ns (@300K)
Lifetime of holes (τ_{p0})	10.0	ns (@300K)
Electron mobility (μ_n)		
Si	1400, 140	$\text{cm}^2/\text{V/s}$ (@300K)
Ge	3900, 390	$\text{cm}^2/\text{V/s}$ (@300K)
Hole mobility (μ_p)		
Si	500, 50	$\text{cm}^2/\text{V/s}$ (@300K)
Ge	1900, 190	$\text{cm}^2/\text{V/s}$ (@300K)
Coefficient of temperature dependence of mobility		
γ_n (Si)	2.42	--
γ_p (Si)	2.20	--
γ_n (Ge)	2.30	--
γ_p (Ge)	1.60	--
Illumination source power density (green light)		
I_c	0.55	$\mu\text{W}/\text{cm}^2$
R	0.5	--
Band gap parameters		
α (Si)	4.73×10^{-4}	--
β (Si)	636.0	K
α (Ge)	4.774×10^{-4}	--
β (Ge)	235.0	K

Simulation results of the temperature dependence of the maximal voltage (V_{max} [V]), the maximal current density (I_{max} [mA/m²], the maximal power density (P_{max} [mW/m²]), efficiency, and fill factor for Si film solar panels is shown in Fig. 2; Fig. 2(a) is for the assumption of bulk quality parameters, while Fig. 2(b) is for the assumption of polycrystalline quality parameters. Comparing Fig. 2(a) with Fig. 2(b), we can find the following:

- V_{max} is insensitive to film quality, and $V_{max} \sim 0.1$ V (@300 K).
- I_{max} is sensitive to the film quality, and $I_{max} \sim 50$ μ A/m² (@300 K) in Fig. 2(b).
- Except for V_{max} , most parameters are sensitive to carrier mobility.
- The efficiency is very low regardless of film quality.

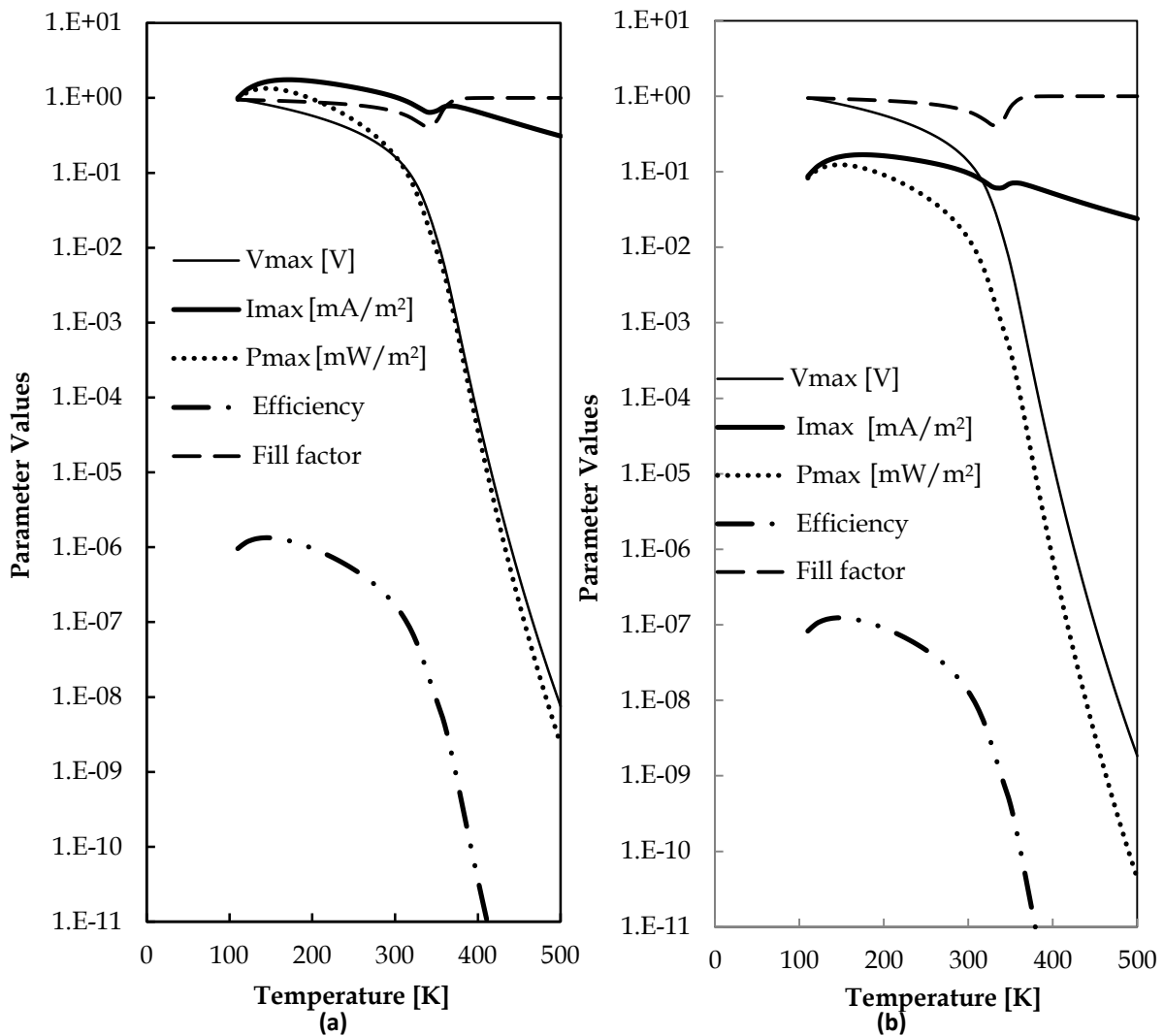


Fig. 2. Temperature dependence of parameters for Si films: a) assumption of crystalline quality; b) assumption of polycrystalline quality.

Simulation results of the temperature dependence of the maximal voltage (V_{max} [V]), the maximal current density (I_{max} [mA/m²], the maximal power density (P_{max} [mW/m²]), efficiency, and fill factor for Ge film solar panels is shown in Fig. 3; Fig. 3(a) is for the assumption of bulk quality parameters, while Fig. 3(b) is for the assumption of polycrystalline quality parameters. Comparing Fig. 3(a) and Fig. 3(b), we can find the following:

- V_{max} is insensitive to film quality, and $V_{max} \sim 1$ μ V (@300 K).

- b) I_{max} is sensitive to film quality, and $I_{max} \sim 0.1 \text{ mA/m}^2$ (@300 K) in Fig. 3(b).
- c) Except for V_{max} , most parameters are sensitive to carrier mobility.
- d) The efficiency is very low regardless of film quality.

A comparison of Figs. 2 and 3 reveals that Ge film devices have much lower performance at room temperature than the Si film devices, but much higher performance at temperatures below 250 K than the Si film devices, which is very interesting.

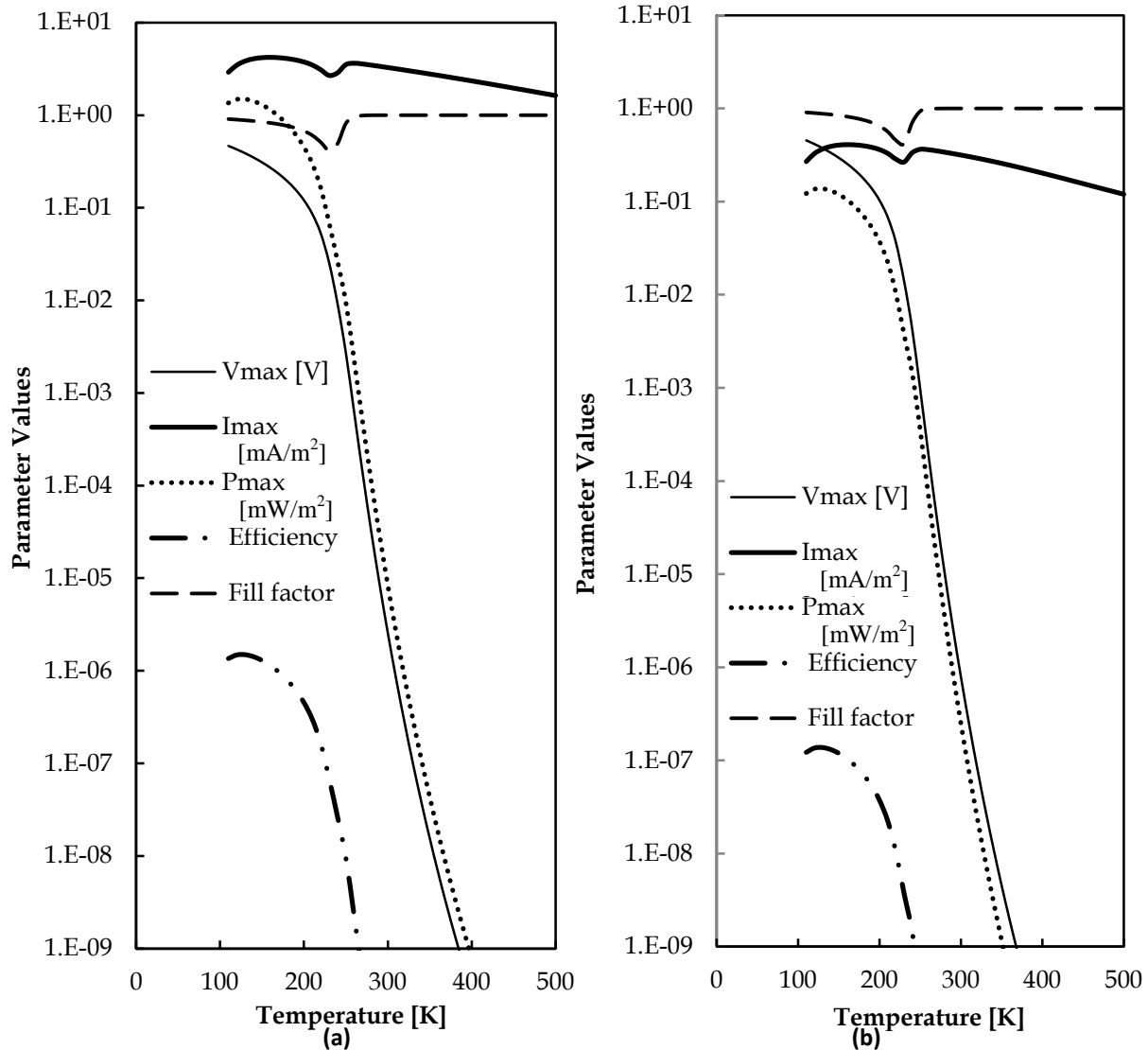


Fig. 3. Temperature dependence of parameters for Ge films: a) assumption of crystalline quality; b) assumption of polycrystalline quality.

Simulation results of the temperature dependence of the excess electron density ($N(x)$ [$/\text{cm}^3$]), the excess hole density ($P(x)$ [$/\text{cm}^3$]), the electron diffusion coefficient (D_n [cm^2/s]), and the hole diffusion coefficient (D_p [cm^2/s]) for Si film solar panels are shown in Fig. 4; Fig. 4(a) is for the assumption of bulk quality parameters, while Fig. 4(b) is for the assumption of polycrystalline quality parameters. Comparing Figs. 4(a) and 4(b), we can find the following:

- a) Excess carrier densities, $N(x)$ and $P(x)$, are rapidly decreased at temperature higher than room temperature.

- b) Excess carrier densities, for the low film quality, are more rapidly decreased at temperature higher than room temperature than for the high film quality.
 c) Generation rates, G_n and G_p , are not sensitive to temperature.

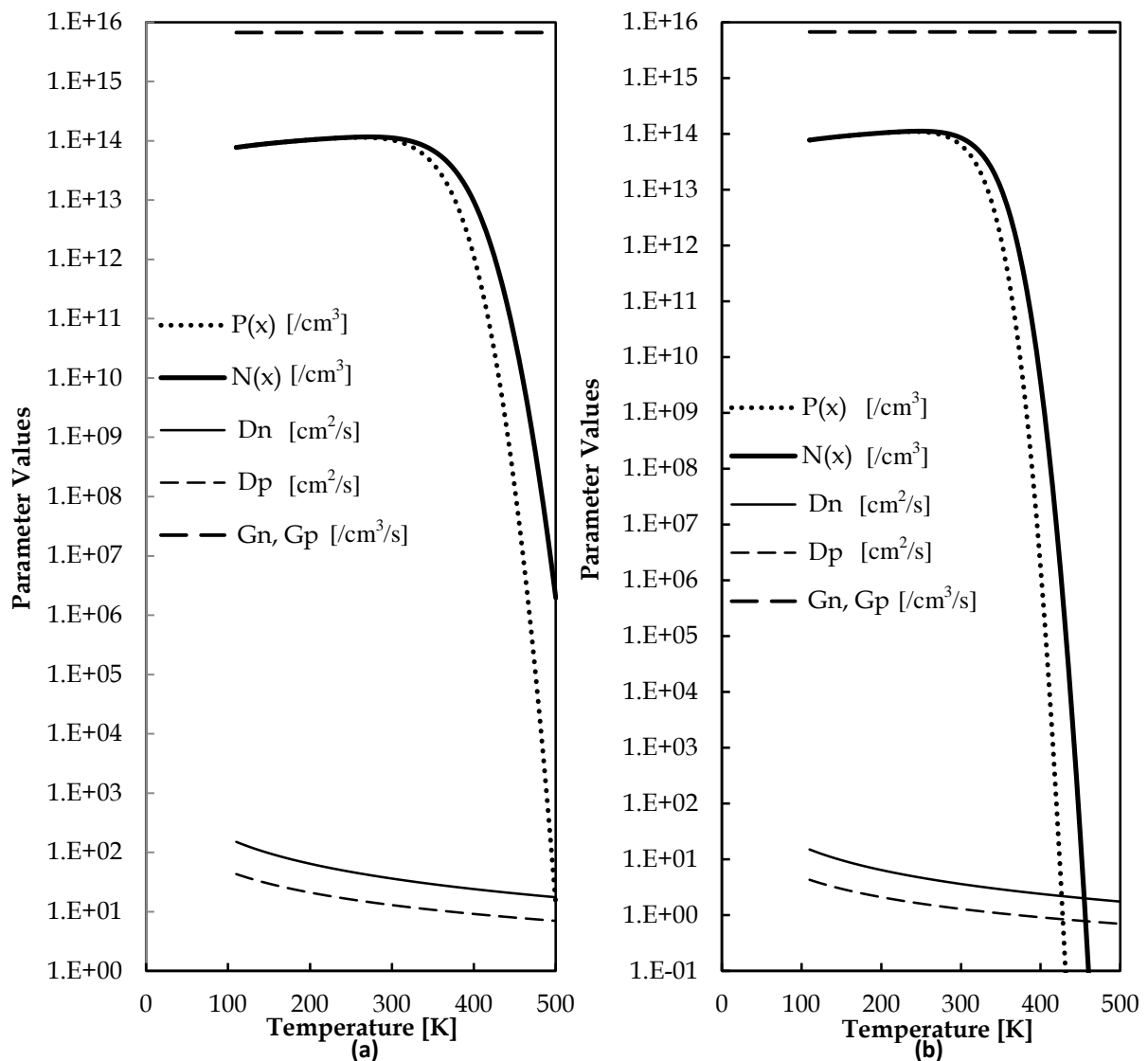


Fig. 4. Temperature dependence of parameters for Si films at $x = L/2$: a) assumption of crystalline quality; b) assumption of polycrystalline quality.

Simulation results of the temperature dependence of the excess electron density ($N(x)$ [cm³]), the excess hole density ($P(x)$ [cm³]), the electron diffusion coefficient (D_n [cm²/s]), the hole diffusion coefficient (D_p [cm²/s]) for Ge film solar panels are shown in Fig. 5; Fig. 5(a) is for the assumption of bulk quality parameters, while Fig. 5(b) is for the assumption of polycrystalline quality parameters. Comparing Figs. 5(a) and 5(b), we can find the following:

- a) Excess carrier densities, $N(x)$ and $P(x)$, are basically insensitive to temperature independent of film quality unlike Si film devices.
 b) Generation rates, G_n and G_p , are not sensitive to temperature.

A comparison of Figs. 4 and 5 reveals that the carrier generation characteristic of the Ge film devices is basically stable against temperature variation unlike the Si film devices.

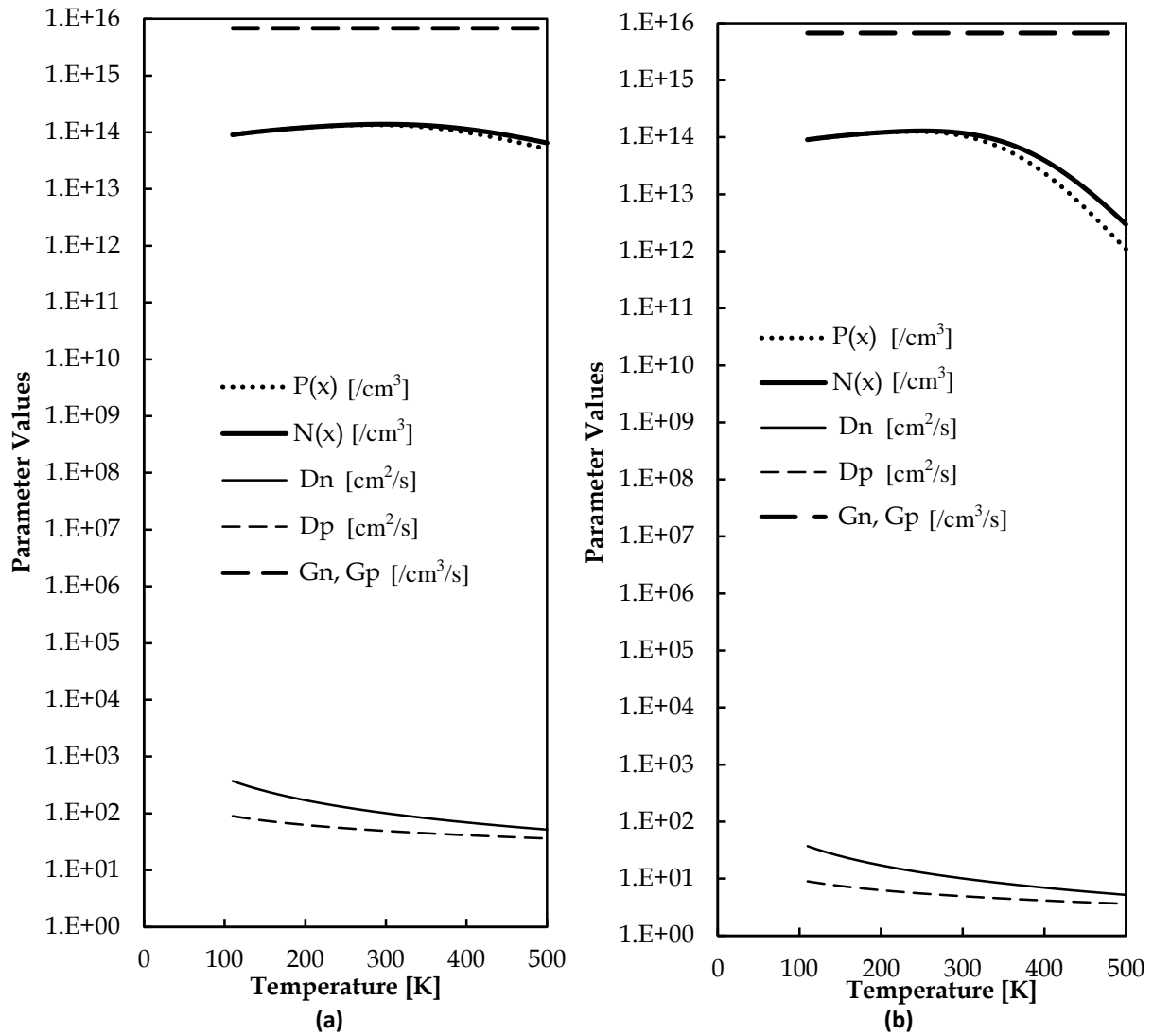


Fig. 5. Temperature dependence of parameters for Ge films at $x = L/2$: a) assumption of crystalline quality; b) assumption of polycrystalline quality.

Since various lateral thin-film pn-junction solar devices have already been investigated, their performances at room temperature are compared in Table 3, where no low-temperature performance data except this study is shown because such experiments and theoretical consideration are missing from past studies. It is known that low-temperature environments yield better performance than room temperature ones [38]. As shown in Table 3, at room temperature, Si-based lateral pn-junction solar devices have comparable performance to chalcogenide solar devices, except for efficiency. Its performance becomes better than that of chalcogenide solar devices except for efficiency at 150 K. On the other hand, the performance of Ge-based lateral pn-junction solar devices is inferior to that of chalcogenide solar devices. At 150 K, however, its performance becomes better than that of chalcogenide solar devices, except for efficiency.

The above simulation results suggest that Si-based multi-stacked thin-film lateral pn junction solar devices formed on a transparent panel can be applied to field sensor devices on the ground at temperatures under 300 K. On the other hand, Ge-based thin-film lateral pn junction solar devices formed on a transparent panel can be applied to field sensor devices on satellites in space because the environmental temperature is lower than 250 K. In these

applications, it is expected that high-efficient peripheral circuits like Schenkel circuits [20, 39] and storage devices will also be required. Such lateral pn junction film devices [5, 6, 24] have already investigated for medical application [27] and others [40]. However, more investigation is needed from the viewpoint of availability of various semiconductor materials.

Table 3. Photovoltaic metrics of lateral p-n junction solar devices (300K).

Material	Wave length [nm]	V _{max} [V]	Fill factor	Efficiency	Ref.
WSe ₂ /MoS ₂	(white light source)	0.22	0.39	0.2	[29]
WS ₂ /WSe ₂	514	0.47	---	---	[33]
MoSe ₂ /WSe ₂	532	0.9	0.2	0.08	[34]
WSe ₂	(white light source)	0.85	0.5	0.5	[35]
WSe ₂	522	0.72	--	--	[31]
bP	640	0.05	0.1	--	[36]
Si	550	0.14 (300K)	0.63 (300K)	1.3x10 ⁻⁸ (300K)	This work
		0.77 (150K)	0.92 (150K)	1.2x10 ⁻⁷ (150K)	
Ge	550	7.9x10 ⁻⁷ (300K)	0.99 (300K)	2.5x10 ⁻¹³ (300K)	This work
		0.29 (150K)	0.84 (150K)	1.2x10 ⁻⁷ (150K)	

4. CONCLUSIONS

This paper proposed covalent-semiconductor-based lateral p-n junction film solar devices and examined their power generation performance under illumination. The comprehensive theoretical model previously proposed by the author was applied to the simulations conducted. The simulations assumed practical device parameters while the physical parameters were taken from a previous study.

Simulation results of the temperature dependence of various performance parameters were discussed for Si films and Ge films. For Si films, the following were revealed:

- V_{max} is insensitive to film quality, and $V_{max} \approx 0.1$ V (@300 K).
- I_{max} is sensitive to film quality, and $I_{max} \approx 50$ μ A/m² (@300 K).
- Except for V_{max} , most parameters are sensitive to carrier mobility.
- The efficiency is very low regardless of film quality.

For Ge films, the following were revealed:

- V_{max} is insensitive to film quality, and $V_{max} \approx 1$ μ V (@300 K).
- I_{max} is sensitive to film quality, and $I_{max} \approx 0.1$ mA/m² (@300 K).
- Except for V_{max} , most parameters are sensitive to carrier mobility.
- The efficiency is very low regardless of film quality.

The Ge film devices have much lower performance at room temperature than the Si equivalent, but that inferiority is reversed at temperatures below 250 K, which is very interesting. A comparison of Si films and Ge films revealed that the carrier generation characteristic of Ge film devices is basically stable against temperature unlike Si film devices.

These simulation results suggest that thin-Si-film lateral p-n junction solar devices in the multi-stacked arrangement formed on a transparent panel are applicable to sensor devices on the ground at temperatures of about 300 K. On the other hand, thin-Ge-film lateral p-n junction solar devices are superior as field sensor devices on satellites in space because the environmental temperature is lower than 250 K; again in the multi-stacked arrangement formed on transparent panels. Since lateral p-n junction film devices are already being

investigated for medical applications and others, it is clear that more investigation is needed from the viewpoint of the availability of various semiconductor materials for future applications.

APPENDIX: Temperature Dependence of Carrier Mobility, Band Gap, and Carrier Lifetime

Temperature dependence of carrier mobility is expressed as [41-43]:

$$\mu_n = \mu_{n0} \left(\frac{300}{T} \right)^{\gamma_n} \quad (\text{A.1})$$

$$\mu_p = \mu_{p0} \left(\frac{300}{T} \right)^{\gamma_p} \quad (\text{A.2})$$

Parameter values (μ_{n0} , μ_{p0} , γ_n , γ_p) are given in Table 2. In addition, temperature dependence of band gap is expressed as [41]:

$$E_G(T) = E_{G0}(0) - \frac{\alpha T^2}{T + \beta} \quad (\text{A.3})$$

Parameter values (α , β) are also given in Table 2. Temperature dependence of lifetime is expressed as [41]:

$$\tau_n = \tau_{n0} \left(\frac{1}{e} \right) \exp \left(\frac{300}{T} \right) \quad (\text{A.4})$$

$$\tau_p = \tau_{p0} \left(\frac{1}{e} \right) \exp \left(\frac{300}{T} \right) \quad (\text{A.5})$$

Parameter values (τ_{n0} , τ_{p0}) are also given in Table 2.

REFERENCES

- [1] W. Shockley, "The theory of p-n junction in semiconductors and p-n junction transistors," *Bell System Technical Journal*, vol. 28, pp. 435-489, 1949.
- [2] S. Sze, *Physics of Semiconductor Devices*, First Edition, Chapter 2, John Wiley and Sons, 1969.
- [3] Y. Omura, *SOI Lubistors*, First Edition, Chapter 2, IEEE Press - John Wiley and Sons, 2013.
- [4] S. Sze, K. Ng, *Physics of Semiconductor Devices*, Third Edition, Chapter 5, John Wiley and Sons, 2007.
- [5] F. Chaves, D. Jiménez, "Electrostatics of two-dimensional lateral junctions," *Nanotechnology*, vol. 29, pp. 275203, 2018.
- [6] F. Chaves, P. Feijoo, D. Jimenez, "2D pn junctions driven out-of-equilibrium," *Royal Society of Chemistry, Nanoscale Advances*, vol. 2, no. 8, pp. 3252-3262, 2020.
- [7] Y. Omura, *Rotor*, Japanese Patent, No. 6470993, 2019.
- [8] Y. Omura, "Theoretical consideration of an optical rotor using a Si pn-junction rod," *Proceedings of MicDat 2019*, Amsterdam, pp. 11-15, 2019.
- [9] Y. Omura, "Potential of nano-scale optical rotor based on a pn-junction wire," *2019 JSAP/IEEE Si Nanoelctronics Workshop*, Kyoto, pp. 87-88, 2019.
- [10] Y. Omura, "Theoretical consideration on potential and scalability of optical rotors based on a p-n junction rod," *IFSA, Sensors and Transducers*, vol. 235, no. 7, pp. 1-8, 2019.
- [11] H. Nathanson, W. Newell, R. Wickstrom, J. Davis, "The resonant gate transistor," *IEEE Transaction on Electron Devices*, vol. 14, no. 1, pp. 117-133, 1967.

- [12] E. Garcia, J. Sniegowski, "Surface micromachined microengine," *Sensors and Actuators A*, vol. 48, pp. 203-214, 1995.
- [13] G. Piazza, V. Felmetger, P. Murali, R. Olsson III, R. Ruby, "Piezoelectric aluminum nitride films for microelectromechanical systems," *MRS Bulletin*, vol. 37, no. 11, pp.1051-1061, 2012.
- [14] X. Yan, M. Qi, L. Lin, "Self-lifting artificial insect wings via electrostatic flapping," *Proceedings of the 28th IEEE International Conference on Micro Electro Mechanical Systems*, Estoril, pp. 22-25, 2015.
- [15] D. Kang, K. Murali, N. Scianmarello, J. Park, J. Chang, Y. Liu, K. Chang, Y. Tai, M. Humayun, "MEMS oxygen transporter to treat retinal ischemia," *Proceedings of the 28th IEEE International Conference on Micro Electro Mechanical Systems*, Estoril, pp. 154-157, 2015.
- [16] N. Inomata, Y. Yamanishi, F. Arai, "Manipulation and observation of carbon nanotubes in water under an optical microscope using a microfluidic chip," *IEEE Transaction on Nanotechnology*, vol. 8, no. 4, pp. 463-468, 2009.
- [17] C. Puleo, H. Yeh, T. Wang, "Applications of MEMS technologies in tissue engineering," *Tissue Engineering*, vol. 13, no. 12, pp. 2839-2854, 2007.
- [18] M. Noda, P. Lorichirachoonkul, T. Shimanouchi, K. Yamashita, H. Umakoshi, R. Kuboi, "Sensitivity enhancement of leakage current microsensor for detection of target protein by using protein denaturant," *IEEE Sensors Journal*, vol. 11, no. 11, pp. 2749-2755, 2011.
- [19] M. Alrashdan, A. Hamzah, B. Majlis, "Design and optimization of cantilever based piezoelectric micro power generator for cardiac pacemaker," *Microsystem Technologies*, vol. 1, pp. 1607-1617, 2015.
- [20] Y. Omura, Y. Iida, "Performance prospects of fully-depleted SOI MOSFET-based diodes applied to Schenkel circuit for RF-ID chips," *Scientific Research, Circuit and Systems*, vol. 4, no. 2, pp. 173-180, 2013.
- [21] S. Lee, J. Jang, Y. Kim, S. Lee, K. Lee, H. Han, H. Lee, J. Oh, H. Kim, T. Kim, M. Dickey, C. Park, "Intrinsically stretchable ionoelastomer junction logic gate synchronously deformable with liquid metal," *Applied Physics Review*, vol. 9, pp. 041404, 2022.
- [22] S. Masum Nawaz, M. Saha, N. Sepay, A. Mallik, "Energy-from-waste: a triboelectric nanogenerator fabricated from waste polystyrene for energy harvesting and self-powered sensor," *Nano Energy*, vol. 104, pp. 107902, 2022.
- [23] P. Kumar, "Recent advancement in different types of solar cell: Role of ZnO nanostructure to improve solar cell performance," *AIP Conference*, vol. 2558, pp. 020035, 2023.
- [24] A. Fournol, J. Blond, A. Aliane, H. Kaya, J. Meilhan, L. Dussopt, "Thermal sensing performances of thin-film lateral PiN diodes at 80 K and 300 K," *The 52nd European Solid State Device Research Conference*, Milan, pp. 285-288, 2022.
- [25] M. Almomani, A. Al-Dmour, S. Algharaibeh, "Application of artificial intelligence techniques for modeling and simulation of photovoltaic arrays," *Jordan Journal of Electrical Engineering*, vol. 6, pp. 296-314, 2020.
- [26] Y. Dabas, M. Tariq Iqbal, "Sizing and analysis of a DC stand-alone photovoltaic-battery system for a house in Libya," *Jordan Journal of Electrical Engineering*, vol. 7, pp. 84-95, 2021.
- [27] 1st USA Medical Battery Conference 2023. <<https://www.sdle.co.il/battery-conferences/1st-medical-battery-conference-2023-as-part-of-mdm-west/>>
- [28] P. Das, S. Behura, S. McGill, D. Raghavan, A. Karim, N. Pradhan, "Development of photovoltaic solar cells based on heterostructure of layered materials: challenges and opportunities," *Emergent Materials*, vol. 4, pp.881-900, 2021.
- [29] M. Li, Y. Shi, C. Cheng, L. Lu, Y. Lin, H. Tang, M. Tsai, C. Chu, K. Wei, H. He, W. Chang, K. Suenaga, L. Li, "Epitaxial growth of a monolayer WSe₂-MoS₂ lateral pn junction with an atomically sharp interface," *Science*, vol. 349, pp. 524-528, 2015.

- [30] S. Memaran, N. Pradhan, Z. Lu, D. Rhodes, J. Ludwig, Q. Zhou, O. Ogunsolu, P. Ajayan, D. Smirnov, A. Fern´andez-Dom´inguez, F. Garcia-Vidal, L. Balicas, "Pronounced photovoltaic response from multilayered transition-metal dichalcogenides pn-junctions," *Nano Letters*, vol. 15, pp. 7532-7538, 2015.
- [31] B. Baugher, H. Churchill, Y. Yang, P. Jarillo-Herrero, "Optoelectronic devices based on electrically tunable p-n diodes in a monolayer dichalcogenide," *Nature Nanotechnology*, vol. 9, pp. 262-267, 2014.
- [32] M. Tsai, M. Li, J. Retamal, K. Lam, Y. Lin, K. Suenaga, L. Chen, G. Liang, L. Li, H. He, "Single atomically sharp lateral monolayer p-n heterojunction solar cells with extraordinarily high power conversion efficiency," *Advanced Materials*, vol. 29, pp. 1701168, 2017.
- [33] X. Duan, C. Wang, J. Shaw, R. Cheng, Y. Chen, H. Li, X. Wu, Y. Tang, Q. Zhang, A. Pan, J. Jiang, R. Yu, Y. Huang, X. Duan, "Lateral epitaxial growth of two-dimensional layered semiconductor heterojunctions," *Nature Nanotechnology*, vol. 9, pp. 1024-1030, 2014.
- [34] P. Sahoo, S. Memaran, F. Nugera, Y. Xin, T. M´arquez, Z. Lu, W. Zheng, N. Zhigadlo, D. Smirnov, L. Balicas, H. Guti´errez, "Bilayer lateral heterostructures of transition-metal dichalcogenides and their optoelectronic response," *ACS Nano*, vol. 13, pp. 12372-12384, 2019.
- [35] A. Pospischil, M. Furchi, T. Mueller, "Solar-energy conversion and light emission in an atomic monolayer p-n diode," *Nature Nanotechnology*, vol. 9, pp. 257-261, 2014.
- [36] M. Buscema, D. Groenendijk, G. Steele, H. Van Der Zant, A. Castellanos-Gomez, "Photovoltaic effect in few-layer black phosphorus pn junctions defined by local electrostatic gating," *Nature Communication*, vol. 5, pp. 1-6, 2014.
- [37] S. Sze, K. Ng, *Physics of Semiconductor Devices*, Third Edition, Chapter 13, John Wiley and Sons, 2007.
- [38] S. Dubey, J. Sarvaiya, B. Seshadri, "Temperature dependent photovoltaic (PV) efficiency and its effect on PV production in the world - a review," *Energy Procedia*, vol. 33, pp. 311-321, 2013.
- [39] Y. Omura, A. Mallik, N. Matsuo, *MOS Devices for Low-Voltage and Low-Energy Applications*, First Edition, Chapter 16, IEEE Press - John Wiley and Sons, 2017.
- [40] H. Pal, S. Singh, C. Guo, W. Guo, O. Badami, T. Pramanik, B. Sarkar, "Lateral p-n junction photodiodes using lateral polarity structure GaN films: a theoretical perspective," *Journal of Electronic Materials*, vol. 52, pp. 2148-2157, 2023.
- [41] S. Sze, *Physics of Semiconductor Devices*, Second Edition, Chapter 1, John Wiley and Sons, 1981.
- [42] S. Kasap, *Principles of Electronic Materials and Devices*, Third Edition, Chapter 5, McGraw Hill, 2006.
- [43] M. Prince, "Drift mobilities in semiconductors 1. Germanium," *Physical Review*, vol. 92, pp. 681-686, 1953.